Mars and Venus Orbiter Spacecraft Electric Propulsion Systems

J. H. MOLITOR* AND K. J. RUSSELL†
Hughes Research Laboratories, Malibu, Calif.

A study was performed to design electric propulsion systems for the Advanced Reconnaissance Electrically Propelled Spacecraft (AREPS) for Mars and Venus planetary mapper missions. The system designs follow previously established mission and spacecraft guidelines and utilize the mercury electron-bombardment ion engine. Basic to the propulsion system design effort was a system design optimization methodology developed earlier. Important study conclusions are that reliable electric propulsion systems with low-weight penalties for reliability are available, the propulsion system can be used for three-axis orientation control, and the ion engine power conditioning system may be used to supply communication system power.

Introduction

PRIOR studies and demonstrations have led to several important concepts or conclusions concerning electric propulsion system (EPS) and spacecraft designs and applications: 1) propulsion system subsystems can be modularized, leading to reliable systems with acceptable weight penalties; 2) modules of a given size can be used as building blocks for various size total propulsion systems, minimizing hardware development programs; 3) electrically propelled spacecraft of a given design can perform a number of missions (i.e., the multimission concept); 4) the use of electric propulsion will, in general, either provide a larger payload for a given launch vehicle or require a small launch vehicle for a given payload; and 5) in the case of missions where large power sources are required at the target planet for high data rate transmission, the addition of electric propulsion is highly desirable.

The last general concept has been most clearly shown in the Mars and Venus planetary mapper missions[1–4] proposed by NASA/Marshall Space Flight Center. Studies of these missions have shown the performance advantages provided by the use of electric propulsion for both the heliocentric trajectory and for maneuvering about the target planet. These studies have been carried to the point where preliminary spacecraft designs have been evolved, and the various subsystems have been defined.

Mission Profiles

Figure 1 outlines the mission profiles. The solar panel power is used to operate the EPS during the heliocentric transfer. At planetary arrival, chemical retropropulsion and spacecraft reorientation are performed to place the spacecraft in near polar orbits. The capture orbits are ~10,000 km for Mars and 3900 km for Venus. The spacecraft then performs a series of descent and mapping operations. Television is used for Mars and side-looking radar for Venus. The 20 kwe available at the planets will be used alternatively to provide high-bit-rate communication and orbit lowering. On the Mars mission the power will also be used to change the inclination of the orbit by use of a side mounted thruster array. Mission parameters are summarized in Table 1.

Presented as Paper 70-1154 at the AIAA 8th Electric Propulsion Conference, Stanford, Calif., August 31–September 2, 1970; submitted October 2, 1970; revision received January 7, 1971. Work performed under NASA Marshall Contract NAS 8-21447.

* Manager, Ion Device Physics Department. Member AIAA.
† Member, Technical Staff. Member AIAA.

Determination of Optimum Module Sizes

A computer program has been written at Hughes which simulates the system mass and reliability as a function of the degree of component modularization and redundancy and determines the optimum system design, i.e., the one which, for a given system reliability, gives minimum system mass.[5]

In their present form, the power conditioning (PC) system designs considered in this study are not able to incorporate arbitrary amounts of redundancy in every individual power supply. If they did, the over-all system reliability could be made as close to one as desired. As a result, the presently modeled thruster-PC configuration has implicit upper limits to which the reliability can be raised. These limits can be evaluated for a given mission as a function of O_T, the maximum number of operating thrusters. Figure 2 presents the maximum attainable configuration reliabilities for the Venus mission. The curve was obtained by performing so-called point reliability evaluations; fixed values of the design variables (degrees of component modularization and redundancy) are input, and the reliability of that design is computed. To find the reliability limits, O_T is set at 1, 2, ... 9 and all the redundancy variables are set at high enough values to raise the reliabilities of their sections essentially to one. The remaining modularization variables were set at typical values, although the reliability limits are independent of these variables because the reliabilities of their sections are raised to one.

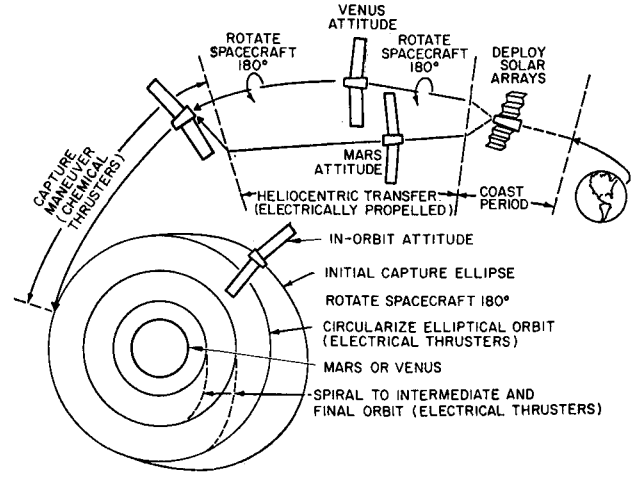

Fig. 1 Mars/Venus surface observation mission profile.

Table 1 Mission parameters

	Mars	Venus
Launch date	Nov. 7, 1977	Dec. 9, 1976
Arrival date	June 16, 1978	June 18, 1977
Launch mass, kg	4331	5132
Mass in planetary orbit, kg	2200	1988
Travel angle, deg	141	235
Launch C_3, km²/sec²	14.5	4
I_{sp}, sec	2778	3158
Thrust at planet, N	0.845	0.815
Power at 1 a.u., kw	40	14.3
Power at planet, kw	19.5	19.9
Arrival C_3, km²/sec²	4.17	2.53
Capture step mass, kg	1493	2845

The interesting feature of the reliability limit curve is that a given system reliability (e.g., $R_g = 0.96$) may be impossible to achieve for some values of O_T (e.g., 4, 5, 7, 8, . . .) regardless of how much optional redundancy is used. Thus, the components (or subsystems) in the system for which additional redundancy is not provided place an upper limit on system reliability. In determining the optimum integer value of O_T for the cases of 0.96 system reliability, it is clear that only the values O_T = 1, 2, 3, and 6 need be considered. Although the behavior R_{max} with O_T is typically decreasing, there is a local rise in the neighborhood of O_T* (equal in this case to 5.8) due to the switch to the more reliable thrusters having diameters less than 30 cm when $O_T > O_T$*. (The inclusion of a design point with $O_T = 6$ is important because it corresponds to a state of the art thruster size.)

The optimum integer value of O_T, and hence the optimum thruster module size, is determined by selecting that one of the possible values O_T = 1, 2, 3, or 6 that makes the total system mass a minimum. By using the optimization computer program's capability to carry out partial system optimizations, the appropriate data required to make the choice were generated. With the variable O_T specified as an input and held fixed at the values 1, 2, 3, and 6, the remaining design variables were determined (using the computer optimization program) so that the system mass is minimum and the system reliability equals 0.96.

Table 2 summarizes the optimum system designs for the Venus mission. The system design with two operating thrusters shows a weight advantage of 11.7 lb over the six operating thruster design. However, the two-thruster design would require the development of new hardware (e.g., a 51.4-cm-diam thruster), whereas the six-thruster design utilizes essentially proven components. For this reason the latter is chosen for the Venus mission.

The thruster failure rate was estimated by combining the failure rates of the thruster's component parts. This method, while presently the only practical method to estimate the thruster failure rate, can only provide a lower bound for the failure rate. Therefore, provision was made in the reliability simulation to multiply the thruster failure rate by a constant (with beam current) factor α. The effect of inaccurate knowledge of α may be illustrated by determining the system reliability for the optimum system design described in Table 2 as a function of α, as shown in Fig. 3. These results reveal that even if the thruster failure rate is five times that estimated, the system reliability has dropped to a still reasonable 0.91.

Table 2 Optimum system designs

	Venus		Mars
O_T, thruster, maximum operating	2	6	15
S_T, thruster, standby	1	2	1
O_B, beam supply, operating	9	9	7
S_B, beam supply, redundant	1	1	0
O_A, accel supply, operating	1	2	1
S_A, accel supply, redundant	0	1	0
S_D, discharge supply, standby	1	1	0
S_{L_1}, line regulator 1, standby	0	0	0
S_I, 5 kc inverter, standby	0	1	0
S_{L_2}, line regulator 2, standby	...	...	0
Thruster module power, kw	9.3	3.1	2.5
Thruster diameter, cm	51.4	30.1	30.1
Beam current, amp	5.3	1.8	1.8
System mass, kg	94.9	100.1	202.0
System reliability	0.96	0.96	0.975

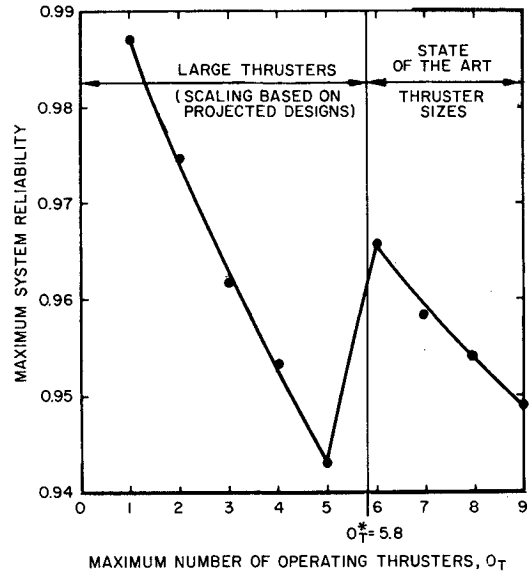

Fig. 2 Maximum attainable reliability (Venus mission).

For the Mars mission, the specific impulse specified by Marshall Space Flight Center is 2778 sec. The mission duration is 5280 hr (220 days). There is a coast period beginning at 1296 hr, during which the EPS is turned off. Optimization for the Mars mission was performed in a manner similar to that for the Venus mission. The design is summarized in Table 2.

Summary of Propulsion System Optimization Results

For the Venus mission, eight 3.1 kw thruster modules are used. As shown by the power profile of Fig. 4, thrusting

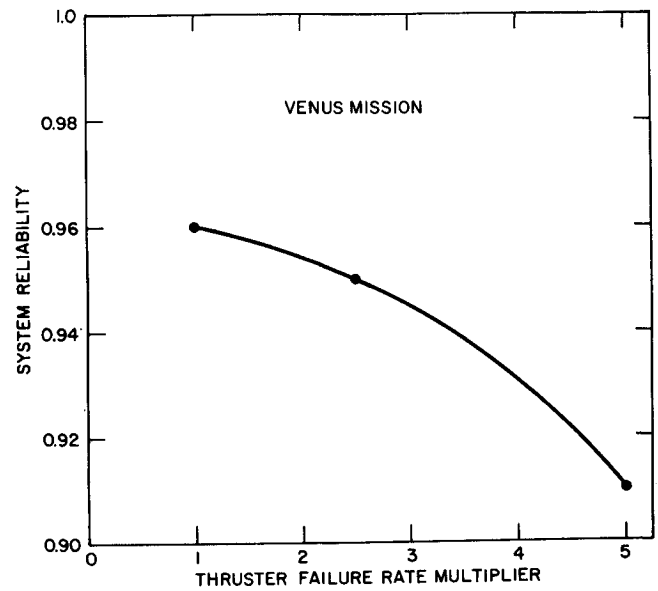

Fig. 3 Sensitivity of propulsion system reliability to thruster failure rate.

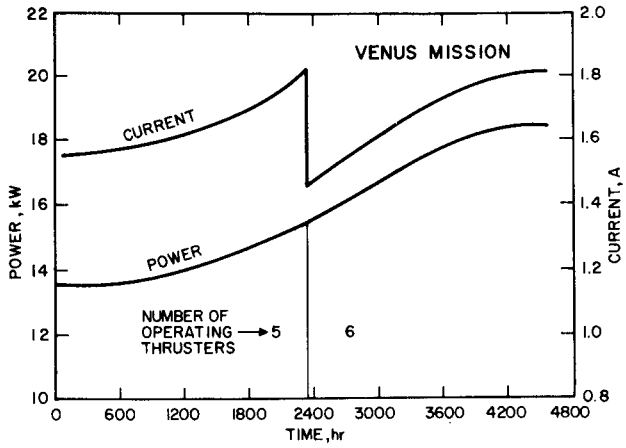

Fig. 4 Thruster module beam current and thruster array input power (Venus mission).

begins with five engines operating at a throttled level of 2.7 kw each. As solar array power increases, en route to Venus, the propellant flow rate and resulting beam current are increased (at constant beam voltage) to deliver the maximum thruster module power (3.1 kw each). At this point an additional thruster is switched on and the six are operated, throttled down at first, until the end of the thrust period. The beam current throttling schedule also is shown in Fig. 4. The two inoperative thrusters are in standby status. Six PC panels are provided, one for each operating thruster. Because there are no standby panels, PC redundancy is built up within each of the supplies that comprises a panel. The numbers of operating and redundant power supply modules that were explicity optimized in the panel design are also shown in Table 2.

For the Mars mission (Fig. 5), thrusting begins with 15 engines (of the total of sixteen 2.5-kw thruster modules) operating at full power. As the solar array power decreases, en route to Mars, the propellant flow rate to the operating engines is decreased until the available power decreases to $\frac{14}{15}$ of its initial value. At this time one operating thruster is switched into standby, and the beam current of the 14 operating thrusters is returned to the maximum value. This sequence of throttling and switching continues until the coast period, during which all thrusters are off. At the end of the coast period thrusting resumes with 10 engines operating at full power (2.5 kw each). Throttling and switching engines into standby then continues to the end of the thrust period. In the interest of commonality and simplicity of design, the

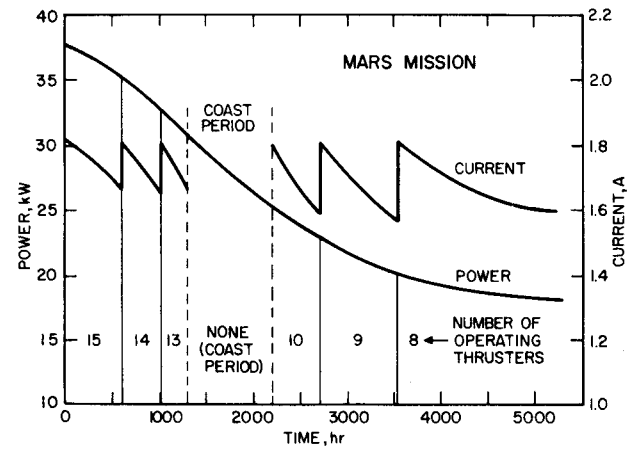

Fig. 5 Thruster module beam current variation and thruster array input power (Mars mission).

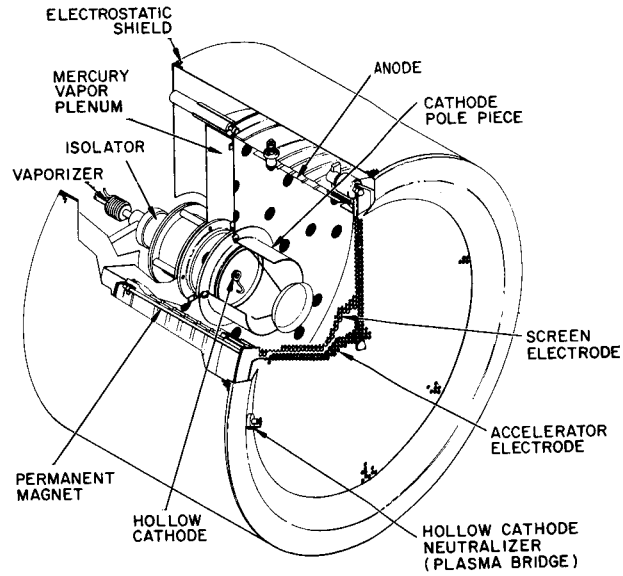

Fig. 6 Hollow-cathode mercury bombardment ion thruster. (Representative of state-of-the-art thrusters).

side thruster array will use thrusters identical to the main thrusters. The array will have eight thrusters, for a total rated power of 20.1 kw.

Design of Electric Propulsion System (EPS) Modules

The optimum EPS designs indicated in Table 2 were specified by describing the values taken by the variables at the optimum. This information, together with that from the scaling studies, can now be used to provide the detailed design of the EPS modules for the two missions. Figure 6 is a schematic of the mercury, hollow-cathode, permanent-magnet, electron-bombardment thruster proposed for these missions. Table 3 gives information pertient to the operation and performance of the thrusters.

The importance of power conditioning (PC) weight was recognized early in the history of electric propulsion. When the large solar cell array emerged as the near-future power source for electrically propelled interplanetary missions, development programs were initiated to obtain suitable lightweight PC. As a result, significant progress has been made in

Table 3 Thruster operation parameters

Parameters	Venus mission	Mars mission
Specific impulse, sec	3158	2778
Input thruster power, w	3088	2511
Thruster beam power, w	2509	1940
Power efficiency (at rated power), %	81.2	77.3
Discharge losses (at rated power), ev/ion	200	200
Propellant utilization efficiency, %	85	85
Accel-decel ratio	2.5	2.5
Beam current, amp	1.818	1.817
Beam potential, v	1380	1068
Thruster power losses (average), w		
Discharge	363.6	363.4
Cathode heater	28.2	28.2
Cathode keeper	18.2	18.3
Accelerator	31.4	24.2
Neutralizer heater	41.3	41.2
Neutralizer keeper	18.2	18.2
Vaporizer and isolator	32.4	32.3
Neutralizer bias	45.4	45.4

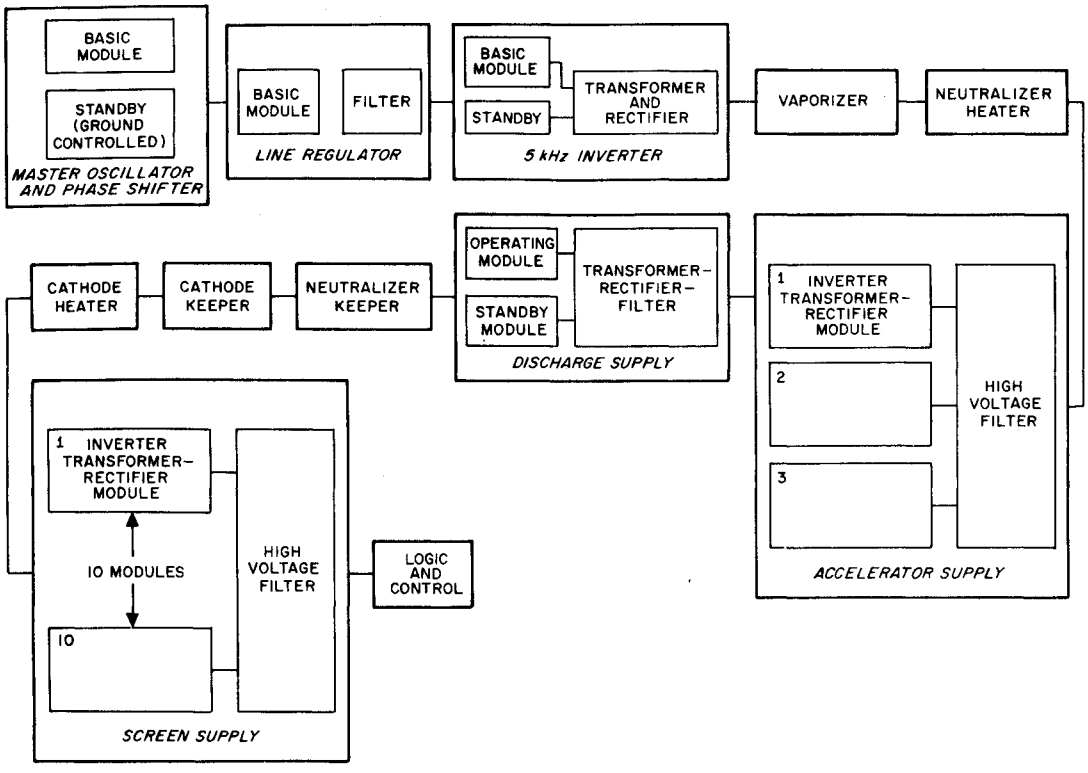

Fig. 7 Power conditioning panel module configuration (Venus mission).

the development of flight prototype electric thruster power conditioning. The type considered here consists of a number of identical panels, each containing all the supplies necessary to operate one thruster. Therefore, eight are used on the Venus spacecraft; 15 on the Mars spacecraft.

The general panel configuration assumed includes arbitary numbers of operating and redundant modules, which are the building blocks of the various thruster power supplies. The panel designs are shown in Table 4, and a block diagram of the panel specified by the computer program for the Venus propulsion system is shown in Fig. 7. The screen supply contains ten operating inverter-transformer-rectifier modules, of which any nine are adequate. The accelerator supply contains three similar modules, of which any two are adequate. One standby module is provided for the discharge supply. For the Mars system, each power supply has one operating module, with the exception of the screen supply (which has 7), and no redundant modules are required.

The use of redundant mercury tanks was not considered, because increasing the reservior subsystem reliability by the use of filled standby tanks incurs an excessive weight penalty, and the use of empty standby tanks does not pay off, because the leak detection mechanisms and valve network necessary to transfer mercury between tanks probably would be less reliable than the tanks themselves. Based on the existing structural members in the spacecraft and the mercury requirements—368 kg for Venus and 682 kg for Mars—it was decided that two tanks and four tanks would be used, respectively. These choices set the individual tank capacity at about 400 lb for both missions. Figure 8 illustrates the tank design.

Table 4 Power conditioning panel specifications

	Mars[a,b]			Venus[a,c]		
Power supply	Power (output), w	Mass, kg	No. of modules operating, redundant	Power (output), w	Mass, kg	No. of modules operating, redundant
Screen (beam)	1986	2.8	7, 0	2555	3.97	9, 1
Accelerator	242.5	0.411	1, 0	313.7	0.877	2, 1
Discharge	363.3	0.859	1, 0	363.6	1.16	1, 1
Cathode heater	28.2	0.157	1, ...	28.2	0.157	1, ...
Cathode keeper	18.2	0.122	1, ...	18.2	0.122	1, ...
Neutralizer heater	41.2	0.203	1, ...	41.2	0.203	1, ...
Neutralizer keeper	18.2	0.122	1, ...	18.2	0.122	1, ...
Line regulator 1	159.5	0.269	1, 0	160	0.269	1, 0
Line regulator 2	260.7	0.378	1, 0	...	[d]	...
5 kHz inverter	148.5	0.240	1, 0	148.6	0.347	1, 1
Vaporizer	32.3	0.196	1, ...	32.4	0.197	1, ...
Panel framework	...	1.76	1, ...	...	2.07	1, ...
Total		7.52			9.49	

[a] Panel efficiency = 0.93.
[b] Panel area = 0.58 m².
[c] Panel area = 0.72 m².
[d] Line regulator 2 not used on Venus spacecraft.

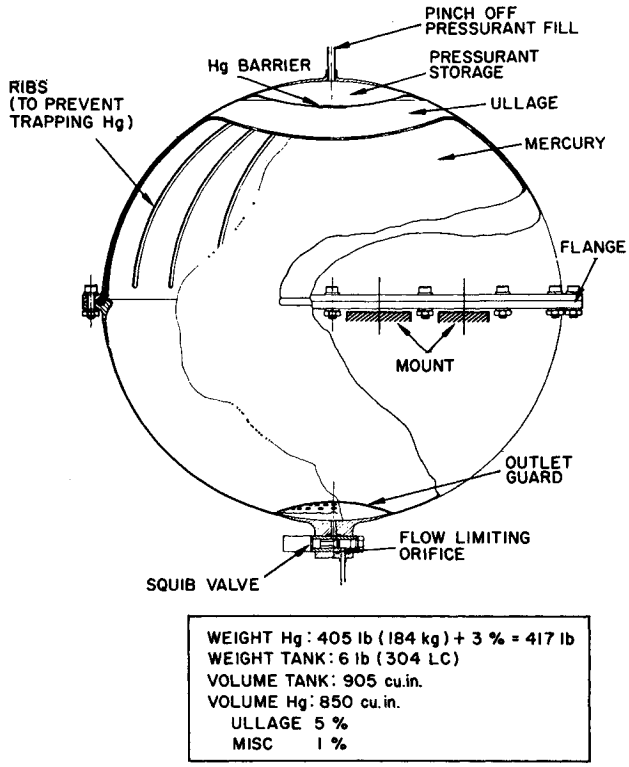

Fig. 8 Positive expulsion mercury propellant reservoir.

Propulsion System/Spacecraft Integration Studies

Once the number and sizes of the EPS modules have been chosen, each of the major subsystems (i.e., thruster array, PC panels, and propellant tankage) must be integrated into configurations that satisfy the mechanical, electrical, and thermal constraints imposed by both the EPS modules themselves and the other spacecraft subsystems. An additional consideration affecting the integration of the ion thruster array into the spacecraft is the possibliity of providing spacecraft orientation control with the prime propulsion system. An evaluation of the requirements of this control function must be made prior to initiation of the thruster array design. Finally, the magnetic and electric field environment produced by the proposed EPS, and the expected impingement of neutral and charged particles on spacecraft surfaces, must be evaluated. To the degree possible, the final design must minimize interactions from these sources.

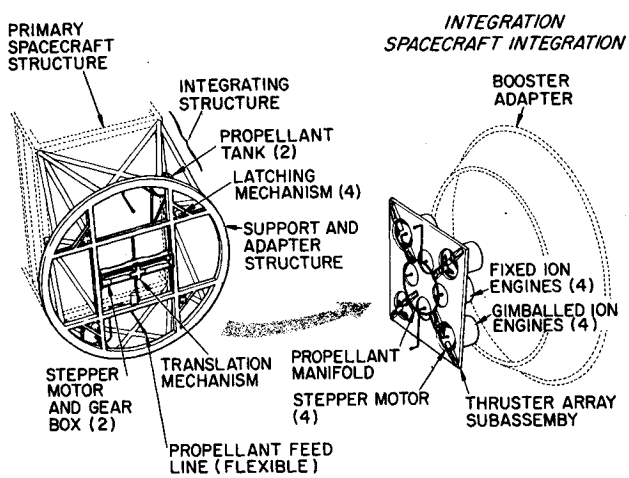

Fig. 9 Mechanical integrating structure (Venus mission).

Spacecraft Attitude Control

In general, the requirements of a spacecraft attitude control system are 1) to orient the net thrust vector of the ion engine array to pass through the vehicle's center of mass, 2) to maintain attitude lock on the sun and star references, and 3) to nullify solar disturbance torque. When these tasks can be reliably and continuously performed by the available ion engine thrust, no supplementary control capability need be provided other than a gas jet system for initial acquisition (or reacquisition) and back-up in case of anomalous performance or meteorite impact. For this reason it is important to consider the various possible techniques for using the prime solar-electric propulsion to achieve three-axis attitude control during the heliocentric thrusting phase of the proposed spacecraft missions.

A system that achieves spacecraft yaw and pitch control through bidirectional orthogonal translation of the ion thruster array and roll control about the thrust vector by gimbaling of outboard thrusters was chosen as the baseline system. (Alternative control techniques which gimbal individual engines or gimbal the entire engine array or which use electrostatic beam deflection to maintain control were considered within the context of the control capability of the baseline system.) For the chosen system, a translator and gimbal thus are incorporated into the over-all thruster array design.

Integration Studies

The EPS/spacecraft integration studies must include considerations of the 1) mechanisms required to provide spacecraft attitude control with the prime propulsion ion thrusters; 2) mechanisms required to maintain the thrust vector through the spacecraft center of mass when a standby thruster is substituted for a failed thruster or when thrusters are turned on or off as the power available from the solar panel varies; 3) structures on which to mount thruster modules, PC panels, and propellant tankage; 4) electrical cabling and switching logic between thrusters (and possibly experiments) and PC panels; 5) piping and manifolds for propellant distribution; and finally 6) the thermal control required to maintain the operating temperatures of the spacecraft subsystems.

Mechanical integration

The integrating structure, as shown in Fig. 9 for the Venus application, consists of a lightweight tubular truss frame designed to carry out the geometric transition from the circular interface with the booster adapter to the rectangular interface on the primary spacecraft structure. On this frame are mounted the PC panels, mercury tanks, electrical power bus, and thruster subassembly translation mechanism. The PC panels are located on three shaded sides of the frame, and the thruster array subassembly is mounted to the array translation mechanism and latching devices on the aft interface. When assembled to the booster adapter, the thruster array is caged for support both axially and laterally by four squib-actuated separation nuts, and the entire thruster assembly is contained within the booster adapter.

The thruster subassembly consists of a mounting tray, thrusters, roll gimbals, translation mechanism interface, caging device interface, fuel manifold and individual flexible thruster feed lines, and electrical harness interfaces. The thrusters are mounted to a rigid lightweight tray with provisions for individual thruster alignment so that it will not be necessary to provide for independent alignment of the complete subassembly. The four outboard thrusters are provided with single-axis gimbals for roll control. The stainless steel mercury tanks (four for the Mars mission and two

for the Venus mission) are supported in the EPS mounting structure near the aft ring. Each tank supplies mercury to the manifold through flexible lines (to accomodate translation).

Electrical integration

Because the missions under consideration require power levels delivered to the experiment of the same magnitude as that to the thrusters and at a time when the main thrusters are off, a significant saving in weight of PC equipment can be realized by sharing as many elements of the power converters as possible. The sharing of thruster power converters with the communication system, which will require the bulk of the experiment power, is particularly desirable. Approximately 75% of the power for the thruster and communication systems shall be provided at similar voltage, enhancing the potential for power conditioning sharing.

Two methods of achieving power converter commonality have been evaluated in this study. One uses relatively small power converters connected in series and/or parallel to generate the higher power and voltages required by the thrusters and experiment loads. The phase and pulse-width of each module are programmed by a control unit to regulate the output voltage to any load. Commonality is achieved with a minimum of additional logic and components, but the modules have not been power matched for highest efficiency. The second method uses the same approach but with one slight modification. A transformer is designed for each experiment load to obtain a power match between the converter modules and load. This arrangement has the potential for improved power conversion efficiency and a more economical use of converter modules, but at the cost of added transformer weight.

Figure 10 shows the conceptual power distribution layout for the Mars spacecraft. To picture the intercabling required, the PC panels, the various electrical loads (front and side thrusters, phased array, scanner, side-looking radar, etc.), and the power switching boxes are shown in approximately the same respective locations as they are found on the spacecraft. Flexible, ribbon-type harnesses are used wherever needed to accommodate translator and gimbal motions. Power from the solar panels is brought to a main bus and divided between the auxiliary spacecraft power conditioning and the 15 PC panels (through one branching harness). The power output of each panel then passes through a switching matrix, which diverts it to the main or side thrusters or the phased array.

Thermal integration

Two important factors in thermal control of a spacecraft are the maximum amount of heat loss that must be radiated and the range over which the heat losses vary during the mission. The first factor, together with the required spacecraft temperature limits, determines spacecraft radiator size; the second determines the complexity of the thermal control system. Considering both factors, and taking solar loading into account, the Mars mission presents a more difficult thermal integration task than does the Venus mission.

Three classes of propulsion system hardware that must be considered here are 1) the thrusters, 2) the PC panels, and 3) all other internally mounted equipment. The spacecraft is sun-oriented about its roll axis, and, consequently, the PC panels mounted on three sides of the vehicles are never illuminated. To minimize thermal interaction between the EPS and the rest of the spacecraft, an adiabatic interface between the EPS and spacecraft has been assumed. The basic electric propulsion subsystem consists of a closed compartment, at one end of which is the thruster array. The thrusters are mounted externally and isolated from the compartment by a multilayer insulation blanket. The sun-facing surface of the compartment is closed by an aluminum shield,

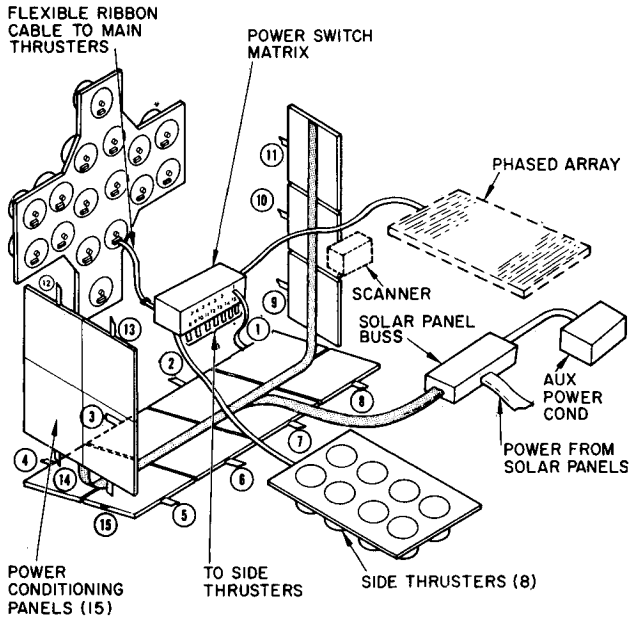

Fig. 10 Power distribution system layout (Mars mission).

black-painted on both sides. Bimetallically actuated louvers on the interior surface of the shield control its effective internal emittance. The shield/louver combination compensates for internal dissipation variations. The other three surfaces of the compartment are formed for the most part by the PC panels, which are painted black on both sides to provide adequate external radiation capability and promote internal coupling. Areas not covered by PC panels are insulated.

Particle and Field Interactions

The primary source of remnant magnetic fields on the spacecraft is the axial permanent magnets mounted on each thruster. The over-all contribution of the complete thruster array can be minimized by alternating the sense of the dipole moments to provide the maximum possible cancellation. Adverse effects can also be minimized by proper location of magnetic-field-sensitive experiments. For extreme cases (e.g., magnetometer on the Mars spacecraft), some magnetic shielding of the experiments from the thruster fields may be necessary. Alternatively, the experiment could be mounted on a boom.

Electric potentials are determined by the equilibrium condition in which no net current leaves the vehicle. The two equilibrium potential differences (and corresponding current flows) of particular interest here are those 1) between the ion beam itself and the spacecraft and 2) between the ion beam-spacecraft system and the space plasma. The present study indicates that no interference of spacecraft electric fields with the science experiments is likely. In fact, because the neutralizer can be biased with respect to spacecraft ground, the spacecraft and space plasma can be made to have the same potential. Because of this spacecraft potential control scientific measurements can be made of the properties of low-energy charged particles. Such measurements are not possible with conventional passive spacecraft whose floating potential is negative with respect to the space plasma.

Continued exposure of various vehicle subsystems (i.e., solar panels, antennas, etc.) to a flux of either direct or charge exchange ions or neutral particles could seriously degrade over-all system performance. For solar electric spacecraft designs[6] that have solar panels downstream of the thruster exhaust plane, a problem may exist. However, for the thruster array locations chosen for the Mars and Venus spacecraft, no component will be located downstream of an operating

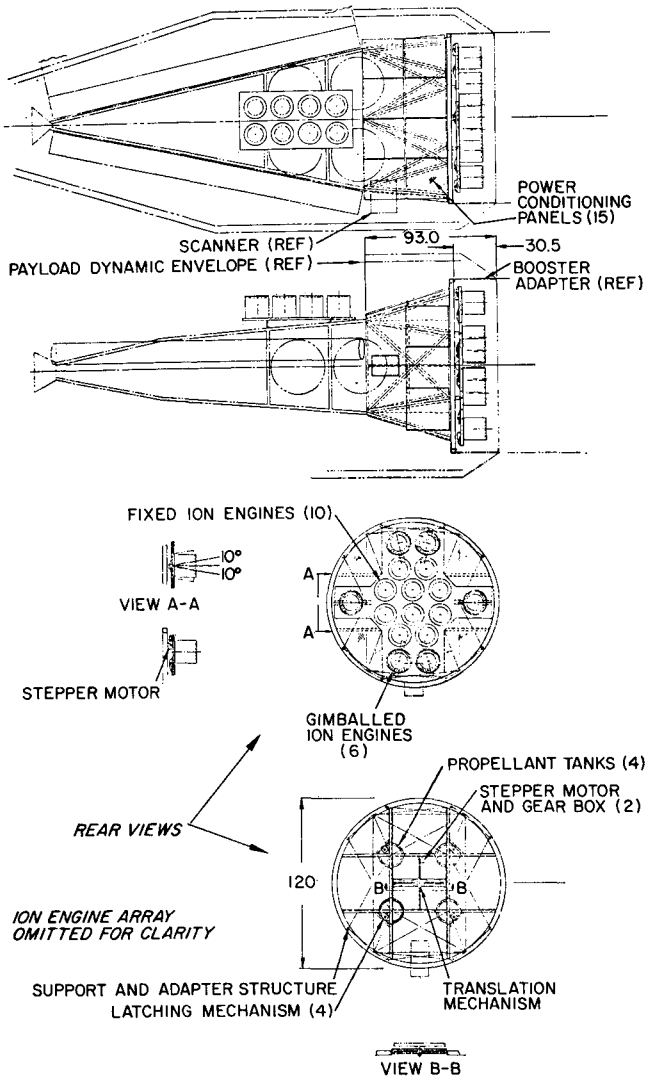

Fig. 11 Mars spacecraft.

thruster, so that beam impingement and neutral mercury deposition can be neglected. Mercury deposition because of charge exchange ions was considered for the Mars spacecraft. The maximum possible flux was estimated to be 10^{11} ions/cm^2-sec. Any arrival rate at the spacecraft will certainly be lower than this estimate. Reference 7 has calculated that at $\sim$1.7 a.u. the worst case arrival rate necessary to produce opaque mercury condensation is $\sim 10^{14}$ atoms/cm^2-sec on the sun side of the solar array. Because the arrival rate for the Mars spacecraft is three orders of magnitude below this critical value, no problems should be expected. For the Venus spacecraft the same conclusion applies, because the temperature is higher and the number of thrusters fewer. In summary, consideration of particle and field interactions indicate that no difficult or unsolvable problems exist in this area.

Spacecraft/Propulsion System Configurations

Because the main spacecraft structural frames appear to be practically identical for both the Mars and Venus vehicles, the EPS assemblies, which comprise thrusters, and thruster/tray or platform, roll gimbals and translation mechanism, fuel tankage valves and lines, PC's, PC switching gear and logic, electric harnesses, EPS integrating structure, and the EPS thermal control system, are constructed so that they can be mounted or demounted as essentially complete units (or separate spacecraft modules), thus facilitating subsystem testing and the associate contractor organizational approach so common in current spacecraft programs. The final spacecraft configuration for the Mars mission is shown in Fig. 11, and Table 5 gives estimates of the EPS assembly weights for Mars and Venus missions.

Table 5 EPS assembly weights, kg

Subsystem	Mars mission		Venus mission	
Thrusters	108	(16)	52	(8)
Power conditioners	204	(15)	82	(6)
Translation mechanism	11		9	
Roll control mechanisms	11	(6)	7	(4)
Latching mechanism	9		8	
Heliocentric transfer fuel	680		368	
Tankage and plumbing	23		13	
Cabling, bus, switching	38		15	
Thermal control, barrier, and wrap	27		18	
Structure	96		70	
Struts		45		32
Rings		13		11
Cross frame		13		9
Thrust array deck		16		9
Miscellaneous attach hardware		9		9
Subtotal	1207		642	
Booster adapter	46		46	
Total (on booster)	1253		688	

Summary and Conclusions

This paper presents the design of electric propulsion systems for the AREPS (Advanced Reconnaissance Electrically Propelled Spacecraft). The designs of these systems were based on the mercury, electron-bombardment ion engine. Along with the detailed design and integration of the propulsion systems, consideration was given to 1) the use of the prime propulsion system for spacecraft orientation control, 2) the switching of the ion thruster power conditioning to the high data rate communication system when the propulsion system is not in use, and 3) the interaction of the propulsion system with other major subsystems. The propulsion system design effort was based on a computer program formulated to define the propulsion system module number and size based on a reliability-weight optimization. Subsequent consideration of system integration and interaction problems then lead to a final system design for each mission. This study has indicated the feasibility and applicability of solar-electric propulsion systems to the AREPS spacecraft concept as originally proposed. Some of the more important conclusions are these. 1) Highly reliable propulsion systems are available with only small weight penalties. 2) The main propulsion system can be used for three-axis orientation control with the incorporation of a thruster array translator (required in modularized systems anyway) and gimbaling of some outboard engines. 3) The use of the ion engine power conditioning system to supply power to the high-data-rate communication system is feasible. 4) All of the major propulsion system subsystems, as well as mechanisms required for attitude control, are either developed or are under development. 5) Interactions between the propulsion system and other major subsystems are minimized by the spacecraft designs proposed.

References

[1] Wood, L. H. et al., "Planetary Photographic Exploration with Solar-Electric Propulsion," AIAA Paper 67-712, Colorado Springs, Colo., 1967.

[2] Wood, L. H., Prasthofer, W. P., and Vachon, R. I., "Photographic Exploration of Mars with Solar-Electric Propulsion,"

Journal of Spacecraft and Rockets, Vol. 5, No. 5, May 1968, pp. 503–509.

[3] Godwin, F. and Dobkins, J. H., "Mission Profile and Baseline Configuration for ARES Space and Military Systems Division," Summary Report, Aug. 1968, Project ARES SMSD-SSL-205, Brown Engineering Research Park, Huntsville, Ala.

[4] Stuhlinger, E. et al., "Versatility of Electrically Propelled Spacecraft for Planetary Missions," *Journal of Spacecraft Rockets*, Vol. 6, No. 10, Oct. 1969, pp. 1162–1170.

[5] Russell, K. J., Seliger, R. L., and Molitor, J. H., "Electric Propulsion Design Optimization Methodology," *Journal of Spacecraft and Rockets*, Vol. 7, No. 2, Feb. 1970, pp. 164–169.

[6] Reynolds, T. W. and Richley, E. A., "Propellant Condensation on Surfaces near an Electric Rocket Exhaust," *Journal of Spacecraft and Rockets*, Vol. 6, No. 10, Oct. 1969, pp. 1155–1161.

[7] Hall, D. F., Newman, B. E., and Womack, J. R., "Electrostatic Rocket Exhaust Effects on Solar-Electric Spacecraft Systems," *Journal of Spacecraft and Rockets*, Vol. 7, No. 3, March 1970, pp. 305–312.

MAY 1971 J. SPACECRAFT VOL. 8, NO. 5

Optimal Station-Keeping at Collinear Points

EDWARD A. EULER*
University of Colorado, Boulder, Colo.
AND
E. Y. YU†
Northwestern University, Evanston, Ill.

An optimal control problem is formulated for stability control at the collinear libration points in the restricted three-body problem. A simple control is derived that can be applied intermittently to establish certain quasi-elliptic orbits around these points predicted by the linear analysis. Numerical simulation results for the Earth-moon system indicate that stability around the collinear points can be maintained for long periods of time using short corrective thrust applications with small fuel consumption.

Introduction

THE restricted three-body problem has been of interest to applied mathematicians for centuries and, in recent years, free trajectories for the restricted three-body model have received considerable analytical and numerical study. The particular locations of the singular or libration points in this system have suggested a number of interesting possibilities for scientific applications.[1–3] Among them are communications, radio astronomy, meteoroid collection, and manned space stations for trips to the moon.

Many studies have been made relating to the periodic orbits around the equilateral points and the sun's perturbation on these motions to see if bounded motion will persist.[4,5] Reference 14 considers the control problem of reaching the librations with zero relative speed. Specific control laws for station-keeping have received little attention because the specific utility of such satellite placements has not yet been defined. For the collinear libration points, however, a much more basic problem is present, that of the instability of small motions around the points. In Refs. 6 and 7 it is shown that all small perturbations away from the collinear points lead to instability in the sense of Liapunov. Therefore, a control effort will be necessary to keep any space probe in the vicinity of the collinear points. In Refs. 8 and 9, some thrust controls are derived that require continuously acting propulsion systems, and, in Ref. 10, a variety of different station-keeping techniques are analyzed.

In this paper we investigate the combination of the favorable effects of the gravitational forces with an intermediate thrust application to keep a space probe in a stable orbit around the collinear points. Here we consider only the circular planar restricted three-body problem, but, of course, the sun, eccentricity, etc. would have to be included for real world applications. An optimal control is derived for low-thrust propulsion systems, not so much to stress the optimal way to maneuver, but for the ease with which a workable thrust control can be derived. Numerical simulation results are presented to illustrate the duration of stable motion and show the validity of the linear analysis.

Presented as Paper 69-906 at the AIAA/AAS Astrodynamics Conference, Princeton, N.J., August 20-22, 1969; submitted August 27, 1969; revision received November 9, 1970.

* Assistant Professor, Department of Aerospace Engineering Sciences; presently Staff Engineer, Space Navigation Technology, Martin Marietta Corp., Denver, Colo. Member AIAA.

† Associate Professor, Department of Mechanical Engineering and Astronautical Sciences, The Technological Institute. Member AIAA.

Analysis

The equations of motion for the restricted three-body problem are the familiar ones written in the rotating coordinate system shown in Fig. 1. These equations are (see, for instance, Ref. 11):

$$\ddot{x} - 2\dot{y} = (\partial\Omega/\partial x) + u_x, \quad \ddot{y} + 2\dot{x} = (\partial\Omega/\partial y) + u \tag{1}$$
$$\Omega = \tfrac{1}{2}[(1-\mu)r_1^2 + \mu r_2^2] + [(1-\mu)/r_1] + (\mu/r_2)$$

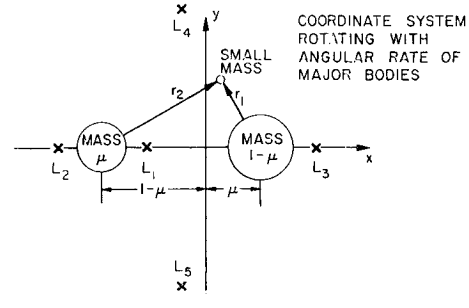

Fig. 1 Coordinate system for the restricted three-body problem and location of libration points.